UNIVERSITAT POLITÈCNICA DE VALÈNCIA

UC DAVIS
UNIVERSITY OF CALIFORNIA

FINAL DEGREE PROJECT

Davis, California, July 2019

PARTICLE SIZE ANALYSIS OF SWEET POTATO CRACKERS DURING IN VITRO DIGESTION

Grado en Ciencia y Tecnología de los Alimentos

Curso 18-19

Autor: Paola Navarro Vozmediano.

Tutor UPV: José Vicente García Pérez.

Tutor externo: Gail M. Bornhost.

Departamento: Biological and Agricultural Engineering (BAE UC Davis) and Escuela Técnica Superior de Ingeniería Agronómica y del Medio Natural (ETSIAMN UPV).

ABSTRACT

PARTICLE SIZE ANALYSIS OF SWEET POTATO CRACKERS DURING IN VITRO DIGESTION

Particle size distribution of food is important to determine the gastric emptying, satiety, and nutrient absorption during gastric digestion. Solid particle breakdown starts during mastication, where ingested solids are mechanically fragmented by the teeth and it continues in the stomach as a result of the peristaltic muscle contractions and the chemical reactions between the matrix and gastric secretions. This process is influenced by the amount of time the food is chewed, exposed to the acidic and enzymatic gastric secretions and how long it spends subjected to the antral contraction waves within the distal region of the stomach.

The following study employed a dynamic in vitro gastric model to analyze the behavior and particle size distribution of different recipes and treatments of sweet potato crackers during gastric digestion. Size distribution was determined every 30 minutes, over/for a total time of 150 minutes of digestion, using Mastersizer 3000 and Image Analysis techniques. Results showed that the number of particles was greater at the end of the digestion and their surface area decreased from the initial sample to the final one. Both aspects were a result of the breakdown processes that occur during digestion. In conclusion, the results of this study proved that Image Analysis and Mastersizer 3000 may be used to quantify the particle breakdown of a food product and it can also help clarify the role of food structure and processing during gastric digestion.

Key words: in vitro digestion; breakdown; crackers; food digestion; particle size.

Author: Paola Navarro Vozmediano.

Davis, July 2019.

Academic tutors: José Vicente García Pérez and Gail M. Bornhost.

RESUMEN

ANÁLISIS DEL TAMAÑO DE PARTÍCULA DURANTE LA DIGESTIÓN IN VITRO DE GALLETAS DE BATATA.

La distribución del tamaño de partícula de los alimentos es importante para determinar el vaciado gástrico, la saciedad y la absorción de nutrientes durante la digestión gástrica. La ruptura de las partículas sólidas comienza con la masticación, donde los sólidos ingeridos son fragmentados por los dientes y continúa en el estómago como resultado de las contracciones peristálticas musculares y las reacciones químicas entre la matriz y las secreciones gástricas. Este proceso es influenciado por la duración de la masticación, por el tiempo en contacto con los ácidos y enzimas de las secreciones gástricas y por el tiempo de permanencia bajo la acción de las contracciones de la región distal del estómago.

El siguiente estudio utilizó un modelo gástrico in vitro dinámico para analizar el comportamiento y la distribución del tamaño de partícula de diferentes recetas y tratamientos de galletas de batata durante la digestión gástrica. Esta distribución fue determinada cada 30 minutos, para una digestión de 150 minutos, mediante el empleo de las técnicas de Análisis de Imagen y Mastersizer 3000. Los resultados mostraron que el número de partículas era mayor al final de la digestión y que el área de partícula se redujo desde la muestra inicial hasta la final. Ambos aspectos fueron resultado de los procesos de ruptura que ocurren durante la digestión. En conclusión, los resultados de este estudio demostraron que las técnicas de Análisis de Imagen y Mastersizer 3000 pueden ser usadas para cuantificar la ruptura de las partículas de un producto alimentario y, además, ayudar a clarificar el papel que tiene la estructura y el procesado del producto en la digestión gástrica.

Palabras clave: digestión in vitro; ruptura; galletas; digestión de alimentos; tamaño de partícula.
Autor: Paola Navarro Vozmediano.
Davis, julio 2019.
Tutores académicos: José Vicente García Pérez and Gail M. Bornhost.

ACKNOWLEDGEMENTS

For seeing in me the perfect candidate for this project, making possible this enriching experience and supporting me during college period, thanks to my tutor, professor and future TFM tutor José Vicente García Pérez.

To Gail Bornhorst for letting me to be part of this project and to all lab mates from 1308 Bainer Hall. Thanks for receiving me as one more, it was a pleasure to work with you during these 4 months.

To my parents Rafael and Inés, my brother Samuel and my family for making this adventure real and being my inspiration and my reason to fight every day.

To my little squad for sharing the hurricane of feelings University causes on us and turn it into amazing nights.

To Enrique for our first coffee.

AGRADECIMIENTOS

Por ver en mí la candidata perfecta para este proyecto, hacer posible esta experiencia enriquecedora y ser mi apoyo durante el periodo universitario, quisiera dar las gracias a mi tutor, profesor y futuro tutor de mi TFM José Vicente García Pérez.

A Gail Bornhorst por dejarme formar parte de este proyecto y a todas las personas de 1308 Bainer Hall. Gracias por recibirme como una más, ha sido un placer trabajar con vosotros durante estos 4 meses.

A mis padres Rafael e Inés, mi hermano Samuel y toda mi familia por hacer real esta Aventura y ser mi inspiración y mis ganas de luchar cada día.

A mi pequeño equipo por compartir el huracán de sentimientos que la universidad nos ha provocado y convertirlo en noches increíbles.

A Enrique, por nuestro primer café.

INDEX

TABLES INDEX

FIGURES INDEX

1. INTRODUCTION

1.1 SWEET POTATOES CHARACTERISTICS AND PROPERTIES.

Due to its unique nutritional and functional properties, sweet potato has become an important topic for many researchers (Wang et al., 2016).

Sweet potato (*Ipomoea batatas L.*) is a perennial tuber. Their perfect climate to grow up is tropical, subtropical and areas with high temperatures. They were discovered in the New World and were introduced into Spain, India, and the Philippines by Spanish explorers in the 15th and 16th centuries. Nowadays, they are worldwide-distributed (Woolfe 1992; Bovell-Benjamin, 2007).

These tubers are nutritious, with low fat and protein content, but also rich in carbohydrates and dietary fiber, vitamins C and A, minerals like iron and potassium and antioxidants such as betacarotene (Mennah-Govela and Bornhorst, 2016). The unique composition of sweet potato gives it many health benefits: anti-oxidative, hepato-protective, antimicrobial, antiobesity, anti-inflammatory, antidiabetic, antitumor and antiaging effects (Wang et al., 2016).

In addition, sweet potato is a versatile food product, they can be cooked in many ways before consumption, such as boiled, steamed, roasted, deep fried, baked and microwaved (Mennah-Govela and Bornhorst, 2016).

Sweet potato can be used as a raw material for crackers. Initially, cracker industry was primarily related with long-term sea travel and war, so as to provide nutritional and emergency food with a long shelf life. The production of crackers was previously based on handmade type, but after the industrial revolution due to mechanical technology, the development of production equipment and technology of crackers, spread across the whole world (Tai-Hua et al., 2019).

In this day and age, a huge percentage of population from many developed countries exhibits malnutrition (having a low micronutrient intake) while simultaneously being overweight (having excess energy consumption). Moreover, links between dietary patterns with health and disease have been strengthened. Due to these links have become popular, consumers have increased their awareness to the functional properties of the foods they consume and have requested the food industry to create new functional food products or food products that contain functional ingredients. On top of that, functional food products may contain certain ingredients (antioxidants or dietary fiber) or they may have a certain structure or formulation in order to modify their functional properties after consumption (Benini et al., 1995; Hertong et al., 1993, Wilson et al., 1998).

As previously mentioned, sweet potato is rich in protein, dietary fiber, vitamins, minerals and some other nutrients that make them a perfect crackers' element. In conclusion, using sweet potato as an ingredient for making crackers may increase the consumption of sweet potato, improve on the disadvantages of single nutritional components of the existing cracker products and enrich the dietary nutrition of

population (Tai-Hua et al., 2019). However, to promote these innovative food products, it is necessary to comprehend the behavior of food during the digestion process, from its initial physical breakdown, to the transformation and absorption of its nutrients. Furthermore, it is important to understand the digestive system parameters (secretion rates, contraction frequency and contraction depth) (Bornhorst et al., 2016).

1.2 GASTRIC DIGESTION PROCESS.

1.2.1 DIGESTION OF FOODS.

During digestion, the first physical change takes place in the mouth. The ingested food is broken down and reduced into small particles that form a cohesive mixture with saliva and the liquid released from the food itself during mastication. Saliva contains the enzyme α-amylase, which will start the digestion by the enzymatically breakdown starch, hydrolyzing α-1,4 glycosidic bonds. The resulting bolus can flow smoothly and safely down along the pharyngeal walls during deglutition (Jalabert-Malbos et al., 2007; Bornhorst et al., 2016). Then, it is transported through the esophagus to the stomach, where gastric digestion starts. During gastric digestion, mechanical and chemical breakdown occur due to both stomach peristaltic contractions and gastric secretions, respectively (Bornhorst and Singh, 2014). The rate of diffusion of gastric fluids into food matrices in the gastric environment may have implications in the overall gastric breakdown as well as absorption of nutrients in the small intestine. In addition, there are factors that may influence the gastric acid diffusion rate, which include food composition, food properties and processing of food (Mennah-Govela et al., 2015).

After gastric digestion, food goes through the small and large intestines where the digested food is mixed to facilitate absorption of nutrients and fermentation (Bornhorst and Singh, 2014). However, to pass through the pylorus and enter the duodenum, the particle size of the food should be less than 1 to 2 mm (Thomas, 2006). Finally, the digestion process ends at the anus (Bornhorst and Singh, 2014).

1.2.2 PHYSIOLOGICAL PROCESSES.

1.2.2.1 Gastric secretions.

Gastric secretions are compound of acid (HCl), enzymes (pepsinogen), mucus, bicarbonate and an intrinsic factor (Barret, 2005). They can be considered to occur in three phases: cephalic, gastric and intestinal. But the major portion of secretion occurs during the gastric phase, when the meal is present in the stomach.

Anatomically, the stomach consists of three regions: fundus, body, and antrum. However, there are only two functional glandular regions: oxyntic and pyloric mucosa. The oxyntic gland mucosa comprises 80% of the fundus and body, while the pyloric gland mucosa comprises 20% of the antrum.

The source of gastric acid secretion is the oxyntic or parietal cell, located in the glands of the fundic mucosa. This cell type is specialized for its function, which is probably the most energetically costly anywhere in the body. High rates of secretion by the parietal cell are sustained by redundant regulatory inputs. Thus, the basolateral membrane of the cell contains receptors for histamine, gastrin, and ACh, which cause potentiated secretion when all are present simultaneously (Di Mario and Goni, 2014). Additionally, stomach secretes 2-3 L of 0.16 N HCl per day (Hersey and Sachs, 1995; Bornhorst and Singh, 2014). In order to maintain the pH of the gastric environment around 1.4 and 2.0, the basal acid secretion rate average between meals is 1mL/min. Conversely, after the ingestion of food the gastric acid secretions may increase to 6 mL/min (Malagelada, et al., 1976; Dressman et al., 1990; Barret 2005).

These secretions are useful to help with nutrients absorption, sterilize food from microbes and contribute to acid-enzymatic hydrolysis of food, resulting in softening of the food matrix (Barret, 2005; Mennah-Govela and Bornhorst, 2016).

1.2.2.2 Gastric motility.

Gastric motility or movement of the stomach walls is vital for digestion (Bornhorst and Singh, 2014). The frequency of stomach muscular contraction is approximately 2 to 3 contractions per minute (Marciani et al., 2001; Kwiatek et al., 2009). However, gastric motility patterns vary between the proximal and distal stomach regions (Bornhorst, 2017). The proximal stomach generates sustained muscle contractions, or tonic contractions of low frequency and amplitude (Lammers et al., 2009). In contrast, the distal stomach experiences phasic, peristaltic muscular contractions (Barret, 2005).

In conclusion, the stomach is responsible for the remaining physical breakdown of the food particles present in the bolus. This breakdown occurs as a result of the pressure and physical forces exerted on the particles from the peristaltic muscular contractions in the gastric.

1.2.3 GASTRIC MIXING PROCESS.

Gastric mixing is nonhomogeneous, and it is the key of the processes during gastric digestion, including the rate of breakdown, pH distribution and gastric emptying (Bornhorst et al., 2014). It is facilitated during digestion through the peristaltic contractions of the muscular walls of the stomach (Bornhorst, 2017).

As a result of mixing, the pH gradually decreases (around to 2.0) resulting in the inactivation of salivary α-amylase (optimum pH 6 to 7) and simultaneous activation of gastric enzymes, such as pepsin (optimum pH 2 to 4).

During mixing, the stomach also acts as a bioreactor, allowing for the hydrolysis of its contents by both acid and enzymes (Bornhorst et al., 2016).

1.3 MODELS OF GASTRIC DIGESTION.

Food digestion can be studied by using either in vitro or in vivo models, both having certain advantages or disadvantages.

On the one hand, in vivo models have many ethical concerns and certain parameters such as gastric viscosity or particle size distribution that may be difficult or impossible to measure. Nevertheless, the advantage of in vivo models is that results are directly applicable to humans. However, variations between individuals may make large differences in responses, and data could be also confused and difficult to analyze (Bornhorst et al., 2016).

On the other hand, in vitro testing allows for rapid screening of food formulations with wide variety of composition and structure, but it also lets the privilege of study all the processes in a controlled environment. In other words, they could control and examinate a huge variety of physical and chemical parameters, in order to simulate the conditions in the gastrointestinal tract.

It is true that food digestion may be such a really hard task to simulate, but many physical and chemical processes may be similar to common unit operations. For example, crushing or grinding may work as a food breakdown during mastication. In addition, digestion models present the enzymatic and pH conditions of mouth, stomach, and intestines and the mechanical and/or hydrodynamic forces to approach the simulation of gastric motility and mixing.

Moreover, the advantages of using in vitro model systems instead in vivo include lower cost, absence of ethical concerns, ability to analyze a wide number of different samples and the opportunity to study the mechanisms of digestion processes individually (Bornhorst et al., 2016).

In conclusion, these methods can assist in predicting food behavior after ingestion permitting better-informed food product design and useful interventions to improve consumer health.

1.4 PARTICLE SIZE DISTRIBUTION.

Particle size distribution of food during gastric digestion is important to determine the gastric emptying, satiety and nutrient absorption. It indicates the amount of physical breakdown that occurred due to the peristaltic movement of the stomach walls in addition to the breakdown that initially occurred during oral digestion. Furthermore, this distribution will be useful to understand the role of food structure and processing in food breakdown during gastric digestion (Bornhorst et al., 2014).

Solid particle breakdown starts during oral mastication, where ingested solids are fragmented by teeth. Besides, several studies have shown a relationship between food particle size after mastication and food type (Bornhorst and Singh 2012).

After swallowing, the physical breakdown of the bolus will occur in the stomach as a result of the peristaltic muscle contractions of the gastric antrum (antral contraction waves (ACWs)) but also chemical breakdown will occur as a consequence of that physical breakdown (Kelly 1980; Meyer1980). Breakage of the food is influenced by the rate at which the matrix is softened by acid and enzymes, plus the extent and rate of overall breakdown. In other words, these processes change by the amount of time a food product is chewed, subjected to the acid/enzymatic gastric secretions and how long it spends subjected to the antral contraction waves within the distal region of the stomach (Bornhorst et al., 2016). Moreover, the particle size of an ingested food and its resistance to breakdown will accomplish an important role in the gastric digestion process (Meyer 1980). For example, while ingested liquids can be quickly emptied from the stomach and move into the small intestines, solid particles need to be physically comminuted to a size smaller than 0.5 to 2 mm before they can pass through the pylorus and exit the stomach. For this reason, if particles have a larger size distribution post mastication and/or have a high resistance to physical breakdown, they will need more time to be able to exit the stomach. In addition, the amount of breakdown that food particles undergo in the stomach may influence digestion and absorption in the intestines by affecting the mass transfer and/or modification of intestinal viscosity (Bornhorst et al., 2014).

2. OBJECTIVES.

The goal of this study the behavior of the sweet potato crackers during a dynamic in vitro gastric digestion and identify the relationship between the breakdown of the crackers and the particle size changes over 3 hours digestion. In order to achieve it some tasks are required:

- Analyze the evolution of particle size during digestion (pellet and creamy layer).
- Comparison of the results between the different recipes and treatments to find out how they may affect to digestion process.

3. MATERIALS AND METHODS.

3.1 SWEET POTATO CRACKERS.

3.1.1. RECIPES.

For this study, different recipes were formulated. After preliminary tests, last version of the recipes is shown in Table 1. Principal ingredients were: Gold Medal All Purpose flour, sweet potato puree (SPP) (Sweet Potatoes distributed by Trader Joe's), salt (McCormik sea salt) and soybean oil (Kirkland Signature, Stratas Foods TM, distributed by Costco Wholesale corporation). In addition, some of the recipes contained protein: Hydrolyzed egg protein (HEP) (Hydrolyzed Egg Whites, Michael Foods, USA) and pea protein (PP) (Roquette Nutralys S85XF).

	No Protein	Hydrolyzed Egg Protein	Pea Protein
Ingredients	Mass (g)	Mass (g)	Mass (g)
Flour	567.4	380.4	324.4
SPP	261.1	261.1	261.1
Salt	2.8	2.8	2.8
Soybean Oil	41.6	41.6	41.6
HEP	-	187	-
PP	-	-	243
Water	-	65	115
Total	872.9	937.9	987.9

Table 1. Sweet potato developed recipes.

Hydrolyzed egg protein had 82.1% protein content while pea protein had 64.9% of protein. The goal for protein recipes was a 25% protein content per cracker after baking and 20% after frying.

3.1.2. SWEET POTATO PUREE.

To prepare sweet potato puree, sweet potatoes were washed, peeled, cut into cylinders (5 mm height) and boiled for 20 minutes on a hotplate. After cooling, they were blended in a food processor (Black and Decker Food Processor, Model: FP2500B, Spectrum Brands, Inc) on high speed in two intervals of 30 s with mixing in between. After preparation, 261.1 g of sweet potato puree was bagged and stored at -18ºC.

3.1.3. COOKING PROCEDURE OF THE CRACKERS.

The first step to make the crackers was thawing the sweet potato puree to 37ºC using a water bath (Isotemp, Fisher Scientific, USA). While it was defrosting, the rest of the ingredients were weighted. After that, dry ingredients were mixed in a stand mixer (Kitchen Aid Stand Mixer, Model: K45SSWH, Color: White) for 1 minute on stir.

The next step was adding the puree and mixing it at speed 2 for 2 minutes. Soybean oil (Kirkland Signature, Stratas Foods TM, distributed by Costco Wholesale corporation) was added after the first minute of mixing. Then, water was incorporated if needed. Finally, speed was increased to 4 for 2 minutes.

Figure 1. Dough for the crackers.

When dough was made, 40 g of it were shaped into spheres and placed onto an iron tortilla press to flat the dough. After that, its thickness was reduced to 1.2 mm using two metal slabs and a rolling pin. Circles were cut out with a cookie cutter (4.5 cm) and were placed on wire racks.

Figure 2. 40g dough's spheres (left) and cut crackers (right).

The total cooking time for each method was selected based on preliminary trials to ensure water activity was ≤ 0.4 after cooking and it is shown in Table 2.

	No Protein		Hydrolyzed Egg Protein		Pea Protein	
	Time (min)	Temp. (ºC)	Time (min)	Temp. (ºC)	Time (min)	Temp. (ºC)
Baked	30	149	30	149	30	149
Fried	12	166	10	166	10	166

Table 2. Cooking treatments for all the recipes.

For baked ones, oven (Single Electric Wall Oven Self-Cleaning with Convection in Stainless Steel, Kitchen Aid) was preheated to 149 ºC and they were cooked for 30 minutes.

For fried ones, 15 minutes in fridge before frying was required. Temperature of the deep fryer (Hamilton Beach, Model: 35034, Type: DF11) was checked to 166 º C. Crackers were flipped after 5/6 minutes depending on the recipe.

Figure 3. HEP fried (1) and HEP baked (2).

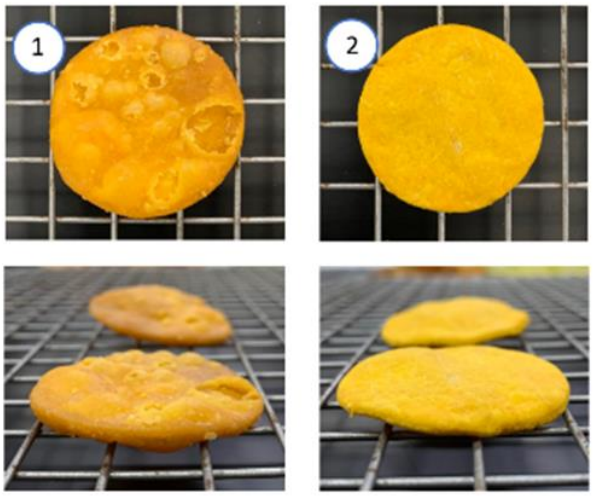

Figure 4. No Protein fried (1) and No Protein baked (2).

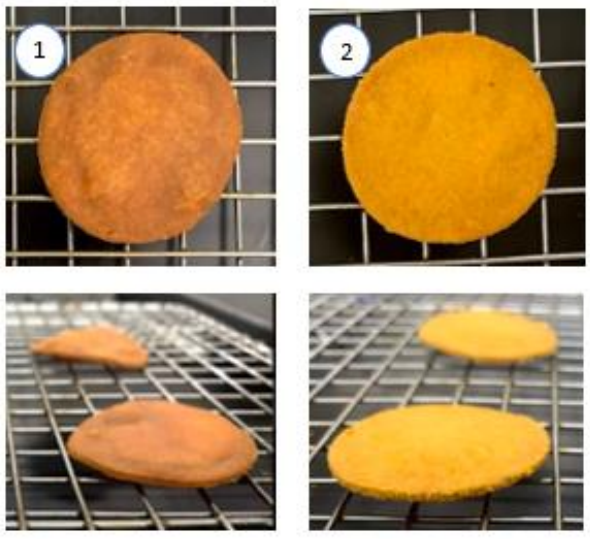

Figure 5. PP fired (1) and PP baked (2).

It was hypothesized that the cooking methods that will be examined would induce structural changes in sweet potatoes, which would modify their uptake of acid and water as well as their propensity for additional structural changes during simulated gastric digestion (Mennah-Govela and Bornhorst, 2016).

3.1.3. INITIAL PROPERTIES.

Texture, moisture content and water activity were defined for each combination of recipe and treatment. Texture was measured as peak force (N) using the TX-XT2 Texture Analyzer provided with a slotted plate and a 7 mm flat cylinder probe at test speed of 1 mm/s and strain 50%. Then, moisture content (% wet basis) was determined gravimetrically in a vacuum oven (Thermo Fisher Scientific, Lindberg/Blue M Vacuum Ovens VO914/ VO1218 /1824) for 22 h at 100ºC. Finally, water activity (aw) was measured using the AquaLab system while

Crackers were made the day before of digestion process. However, an overtime study of their properties' stability was executed (Annex 1) in order to know if they could be made more in advance.

3.2 SIMULATED DIGESTION.

To begin with the experiments, No Protein Baked SPC were analyzed in this study. Next step will be the digestion of the rest recipes and treatments.

3.2.1 SIMULATED SALIVA FORMULATION.

For simulated saliva were needed: 1 g/L Mucin (Sigma- Aldrich, MO, U.S.A.), 1.41 g/L KCl (Fisher Science Education, IL, U.S.A.), 0.63 g/L KH_2PO_4 (Fisher Science Education, IL, U.S.A.), 1.43 g/L $NaHCO_3$ (Fisher Science Education, IL, U.S.A.), 0.04 g/L $MgCl_2 (H2O)_6$ (Fisher Science Education, IL, U.S.A.), 0.01 g/L $(NH_4)_2 CO_3$ (Fisher Science Education, IL, U.S.A.), 0.221 g/L $CaCl_2(H_2O)_2$ (Fisher Science Education, IL, U.S.A.) and 1.18 g/L α-amylase (Bacillus subtilis, MP Biomedicals, Catalog Number 100447, activity of 160,000 BAU/g, Santa Ana, CA, U.S.A.). All ingredients were mixed in a beaker filled with deionized water. Finally, pH was checked and adjusted to 7 (Minekus et al., 2014; Roman, Burri, and Singh, 2012; Bornhorst and Singh, 2013).

3.2.2 GASTRIC JUICE AND LIPASE FORMULATION.

For simulated gastric juice were needed: 1.5 g/L Mucin (Sigma-Aldrich, MO, U.S.A.), 0.643 g/L KCl (Fisher Science Education, IL, U.S.A.), 0.153 g/L KH_2PO_4 (Fisher Science Education, IL, U.S.A.), 2.625 g/L $NaHCO_3$ (Fisher Science Education, IL, U.S.A.), 3.452 g/L NaCl (Avantor Performance Materials, PA, U.S.A.), 0.031 g/L $MgCl_2 (H2O)_6$ (Fisher Science Education, IL, U.S.A.), 0.06 g/L $(NH_4)_2 CO_3$ (Fisher Science Education, IL,

U.S.A.) , 0.022 g/L $CaCl_2(H_2O)_2$ (Fisher Science Education, IL, U.S.A.) and 2000 U Pepsin from porcine pancreas (Sigma-Aldrich MO, U.S.A.). All ingredients were mixed in a beaker filled with deionized water. Also, pH was checked and adjusted to 1.2 (Minekus et al., 2014; Roman, Burri, and Singh, 2012; Bornhorst and Singh, 2013).

For simulated lipase formulation were needed: 0.634 g/L KCl (Fisher Science Education, IL, U.S.A.), 0.136 g/L KH_2PO_4 (Fisher Science Education, IL, U.S.A.) , 8.925 g/L $NaHCO_3$ (Fisher Science Education, IL, U.S.A.) , 2.808 g/L NaCl (Avantor Performance Materials, PA, U.S.A.), 0.084 g/L $MgCl_2$ $(H2O)_6$ (Fisher Science Education, IL, U.S.A.), 0.088 g/L $CaCl_2(H_2O)_2$ (Fisher Science Education, IL, U.S.A.), 10 g/L Bile extract (Sigma-Aldrich MO, U.S.A.) and 2.4 g/L Pancreatin (Sigma-Aldrich MO, U.S.A.). All ingredients were mixed in a beaker filled with deionized water. In addition, pH was checked and adjusted to 4.5 (Minekus et al., 2014; Roman, Burri, and Singh, 2012; Bornhorst and Singh, 2013).

3.2.3 ORAL AND GASTRIC DIGESTION PROCEDURE.

As mentioned, oral digestion starts with the physical breakdown of food. A food processor (Black and Decker Food Processor, Model: FP2500B, Spectrum Brands, Inc) was employed to simulate the mastication. After that, crackers were sieved with 2.36 mm and 0.85 mm sieves. For masticated sample, 120 g of the 0.85 mm particles were used. Then, masticated crackers were mixed with 90 g of saliva for 30 s.

So as to reproduce gastric digestion, a Human Gastric Simulator (HGS) (shown in Figure 6) was employed. The first step of gastric digestion was to introduce the sample in to the HGS bag where 70 ml of gastric juice were already placed to simulate human empty stomach conditions. In addition to recreate real digestion environment, a heat and a fan were installed to maintain the temperature at 37ºC, and plastic walls covered the simulator.

At the same moment the sample was entered to the bag (Figure 7), the pumps were activated. Syringe pump was used for lipase at speed of 0.5 ml/min and gastric juice, placed in a 400 ml beaker, was added by a peristaltic pump at speed of 3 ml/min. After HGS was working, samples were taken every 30 minutes.

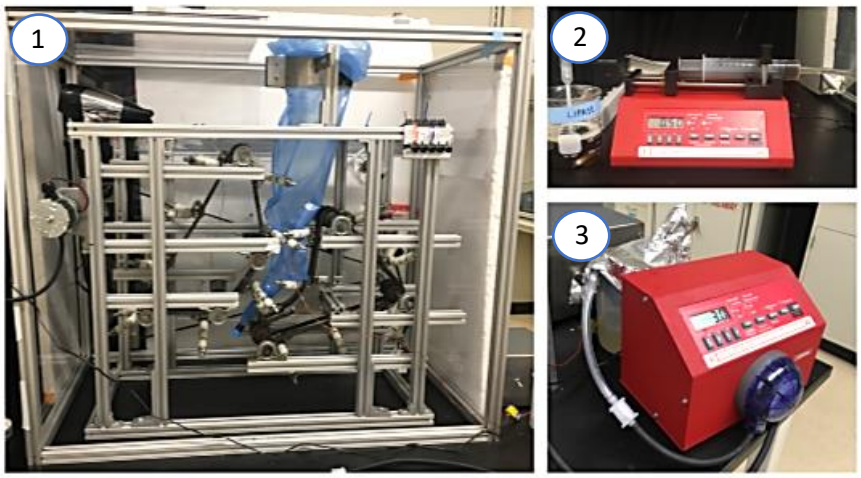

Figure 6. Human Gastric Simulator (HGS) (1); syringe pump for lipase (2) and peristaltic pump for gastric juice (3).

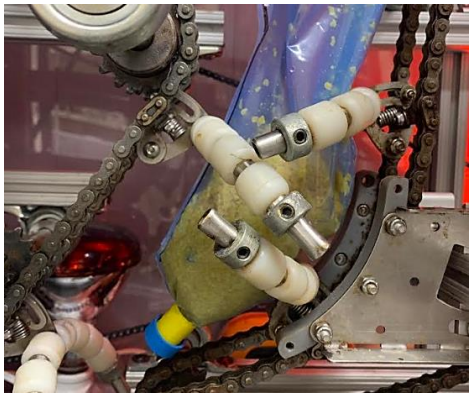

Figure 7. Sample assembled in the HGS bag.

In this experiment, 2.5 hours (150 min) were applied for gastric digestion. An aliquot of each timepoint sample was taken to evaluate moisture content of whole digesta. The rest of the sample was centrifuged for 3 minutes at 4122 x g speed.

As a consequence of centrifuge, different layers appeared (presented in Figure 8). On the top, an oily thin layer was found. Then there was the supernadant, the creamy layer which was analyzed by Mastersizer for particle size and the pellet, which was used for study its moisture content and its particle size by image analysis technique.

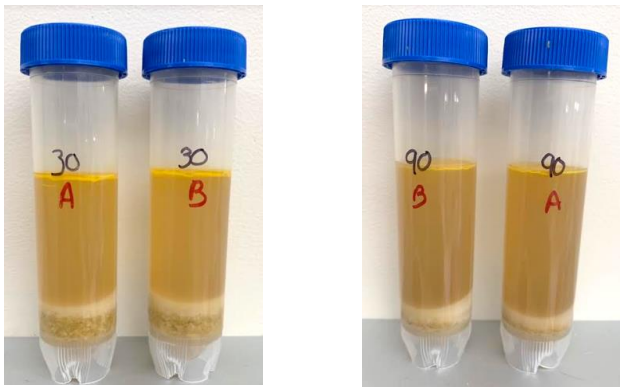

Figure 8. 30 min and 90 min samples after centrifuge.

3.3 SWEET POTATO BEHAVIOR DURING GASTRIC DIGESTION.

3.3.1 MOISTURE CONTENT.

In the same way as initial properties, moisture content was determined gravimetrically in a vacuum oven (Thermo Fisher Scientific, Lindberg/Blue M Vacuum Ovens VO914/ VO1218 /1824) for 22 h at 100ºC. Two to four pans (A, B (whole digesta), C, D (pellet)) per timepoint were labeled and introduced in the oven to pre-dry for 45 min. Their masses were recorded, and samples were put into each pan. The total mass was written again. Finally, after 22 h, the pans were weighed.

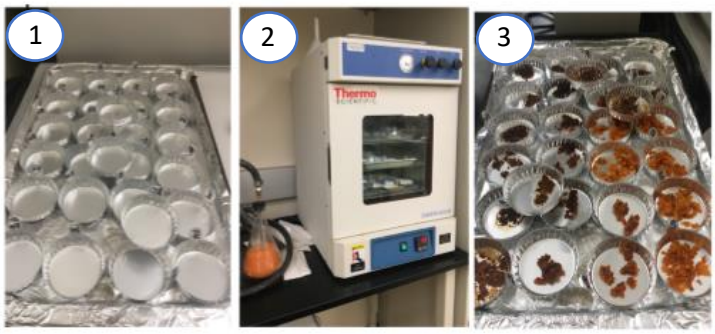

Figure 9. Labeled pans for samples of each time point (1); vacuum oven (2); samples after 22 h at 110ºC (3).

3.3.2 PARTICLE SIZE DISTRIBUTION.

3.3.2.1. Image Analysis.

The needed equipment for image analysis is shown in Figure 10. As seen, it consists in a camera (Canon RebelSL1 EOS 100D) at height of 47 cm, two lamps, a lightbox and a computer.

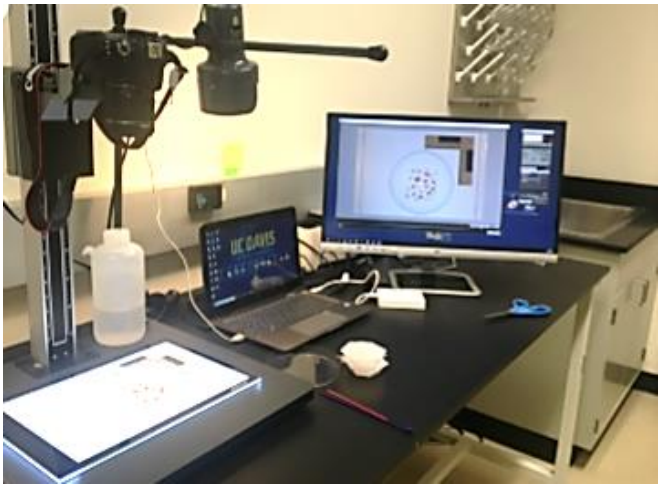

Figure 10. Equipment for Image Analysis.

The first step for image analysis was setting the computer and turning on the camera, the lamps and the lightbox. The lightbox needed to be at high level and after turning on the lights it was very important to make sure there were no shadows or glare. If they appeared, the picture was retaken. Additionally, a scale was placed on the lightbox allowing the computer converting particle sizes from pixels to mm^2.

1 g of each timepoint sample was used for this analysis and it was kept in a weighting boat. After that, the samples were placed in a petri dish illuminated from the bottom by the lightbox and particles were separated with a spatula. Initial and saliva timepoints were imaged without addition of water. For the rest of timepoints, osmosis reverse (RO) water was added to the weighting boats and they were shaken in the orbital shaker (GeneMate, BioExpress, BT30-GM Low Speed Orbital Shaker, Model: 16020015) for 10 minutes. RO water was added to avoid the yellow background and taking more clear pictures. In addition, shaker was used to separate the different particles without provoking more breakdown.

For each sample, 6 to 8 pictures were taken (Figure 11). Different petri dishes were used to separate the particles, to avoid any hidden particles and making sure separation was perfectly done.

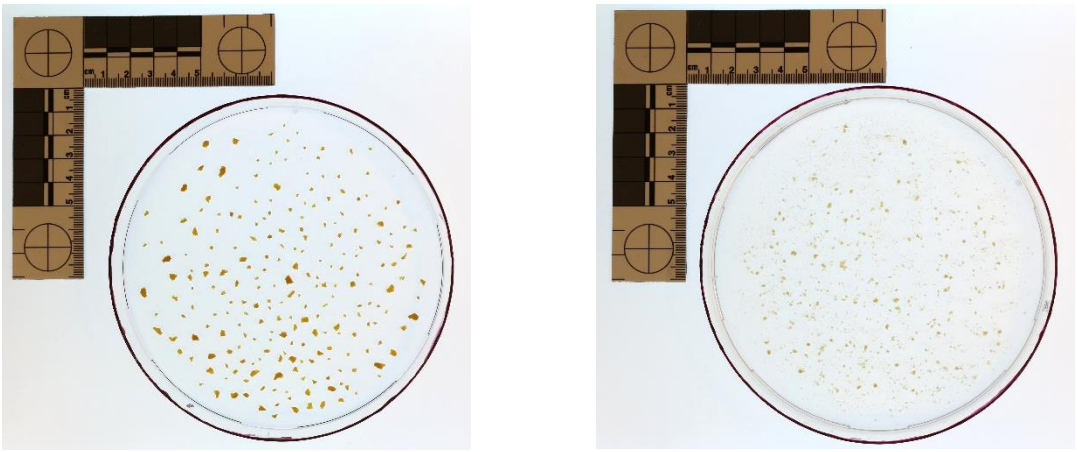

Figure 11. Picture taken before digestion (0 min) (on the left) and picture after 90 min digestion (right).

After pictures were taken, Matlab program R2018a (MathWorks, Natick, Mass. U.S.A.) processed them. A specific code was employed to run the images. It generated 3 new different images for each timepoint and an Excel with the number of particles and its particle size area, converted from pixels to mm^2. Finally, another code was used to run the values in the Excel to fit the cumulative percentage of particle area to the Rosin-Rammler distribution function:

$$C_{area} = 1 - e^{(-(\frac{x}{x_{50}})^{b}.\ln(2))}$$

C_{area} is the cumulative area percentage (0% to 100%) of a particle with x size (mm^2). Additionally, x_{50} is the median particle area (mm^2) and b is a dimensionless constant representing the broadness of the distribution (0 to infinity). A larger value of

b refers to a narrower distribution spread. Both parameters of the model were determined using Matlab codes (Bornhorst et al., 2013).

3.3.2.2. Mastersizer 3000.

In order to analyze the creamy layer particle size, Mastersizer 3000E with Hydro EV dispersion unit (shown in Figure 12) was employed.

Figure 12. Mastersizer 3000E Hydro EV.

Mastersizer uses the technique of laser diffraction. A static light scattering is utilized to measure particle size distribution in an emulsion or suspension. The sample is dispersed in dispersing fluid and is fed through the analysis chamber in the optical bench. As the particles flow through the optical bench, they pass between two glass panes (shown in Figure 13). The instrument sends a laser beam through the windows and the angular variation in intensity of the scattered light is measured. Large particles scatter light at small angles relative to the laser beam and small particles scatter light at large angles, as seen in Figure 14. The detectors assess the scattering pattern created when the beam passes through the particulates, and the instrument translates this into a particle size distribution reported as a volume equivalent sphere diameter (Malvern Mastersizer 3000 manuals). This instrument is suitable for measuring particles with sizes between 0.1 to 1000 µm.

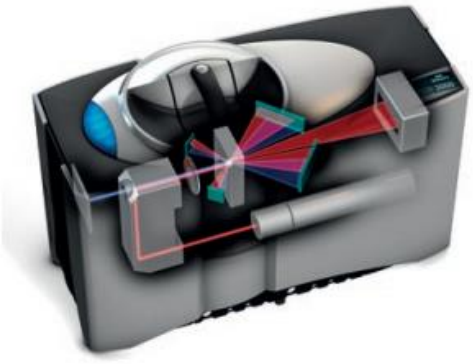

Figure 13. Mastersizer laser diffraction technique.

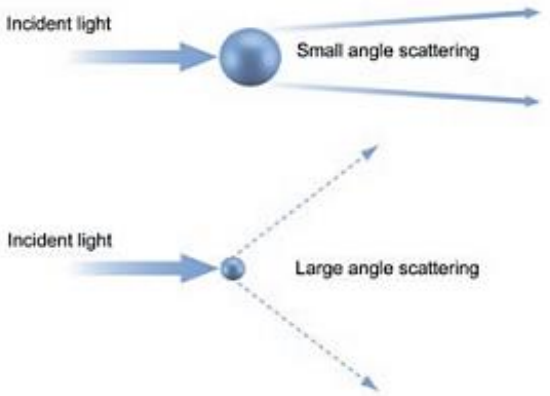

Figure 14. Behavior of the different particle sizes.

The first step of the analysis was to establish the experimental conditions:

- Non-spherical particles.
- 2500 rpm.
- Deionized water as dispersant (1.33 refractive index).
- Sweet potato (1 particle absorption index; 1.53 particle refractive index).
- 10 measurements for each replicate.
- Quick cleaning.

In addition, all the samples were mixed with 3 ml of deionized water to be easily dropped and quickly detected by the equipment.

When the program was set up, drops of the first sample were added in the 600 ml deionized water dispersant beaker until the detector range signal of the program was appropriate. Each sample of each timepoint was evaluated for 3 times. After each replicate, cleaning was required, and instructions were provided by the software. Related to the results, the program generated an Excel sheet with all the values to be analyzed.

4. RESULTS AND DISCUSSION.

4.1. INITIAL PROPERTIES.

Water activity, moisture content and texture were defined for each combination of recipe and treatment. Comparison between them is shown in Figure 15, 16 and 17.

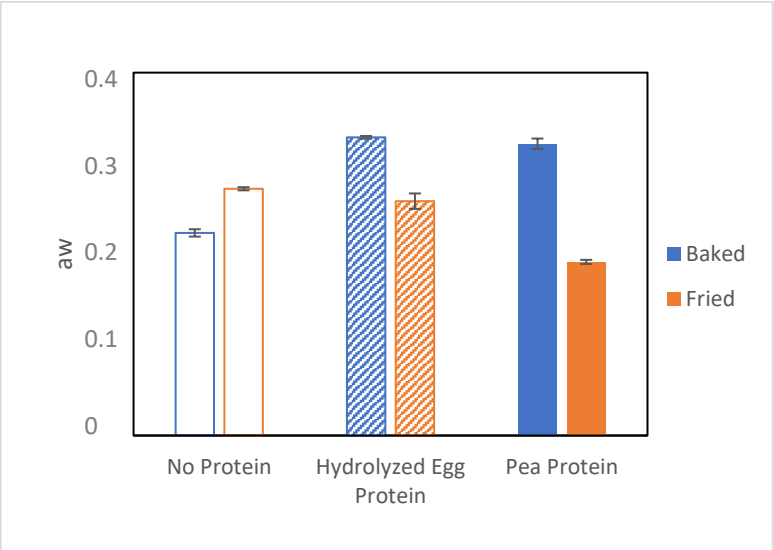

Figure 15. Water activity comparison.

Referring to water activity, the goal was not surpassing 0.4 value and all the crackers satisfy it.

Generally, baked technique has higher aw in all recipes except the control one with no protein. That difference between no protein fried and no protein baked may be related to the oil absorption during frying or because the samples did not wait enough to equilibrate before measuring them.

Protein crackers have higher aw values compared to no protein ones. The water addition on the protein recipes may explain this difference.

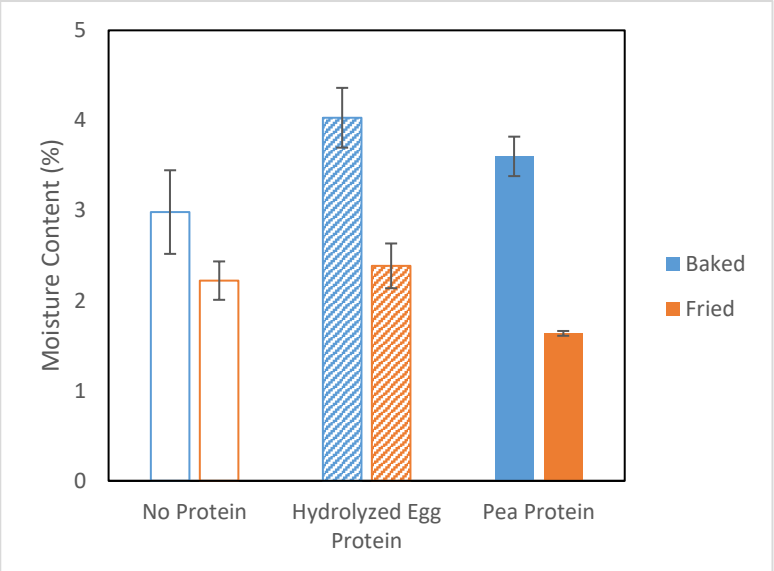

Figure 16. Moisture content comparison.

Like water activity results, moisture content is higher on baked crackers. In addition, its low aw value, would allow the product to have a long shelf-life.

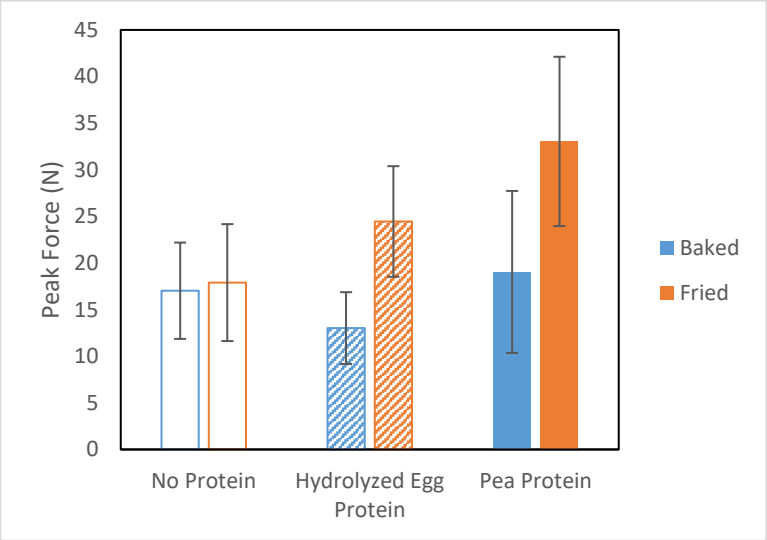

Figure 17. Texture comparison.

About texture, fried technique shows higher values compared to baked method. Moreover, pea protein fried crackers are the hardest ones. Texture is an important property to measure because it will influence the structural breakdown by food resistance to fracture and erosion, as well as influencing the rate of acid diffusion into the food matrix (Bornhorst et al., 2015).

In this study No Protein Baked SPC were analyze. Initial properties of them, shown in Table 3, were determined the day before of the digestion.

aw	Texture (N)	Moisture content (% wet basis)
0.34 ± 0.02	25.67 ± 6.65	2.62 ± 0.23

Table 3. Initial properties of SPC for digestion.

4.2 GASTRIC DIGESTION.

4.2.1 MOISTURE CONTENT.

Moisture content evolution during in vitro gastric digestion is shown in Figure 18. The whole digesta of sweet potato crackers had a higher increase in moisture overtime than the pellet. Initial moisture content was 2.95 ± 0.19 % wet basis increasing to 93.17 ± 0.18 % wet basis for whole digesta. On the other hand, pellet moisture content was 64.81 ± 0.23 % wet basis increasing to 73.75 ± 0.00 % wet basis after 2.5 hours digestion.

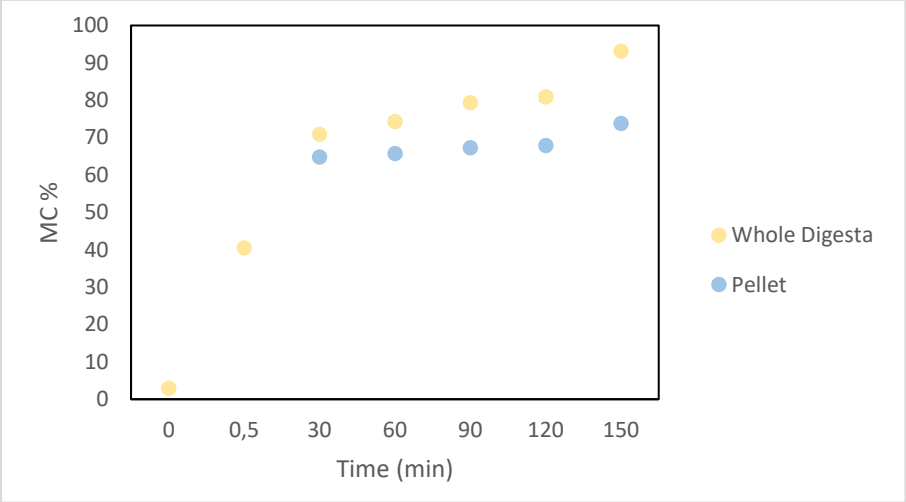

Figure 18. Moisture content (wet basis) evolution during simulated gastric digestion.

The quantity of water absorption may be related with the cooking method and the food matrix. New simulated digestions will figure out this hypothesis by using the different recipes and treatments already mentioned before and comparing the results with the ones obtained in this study.

4.2.2 PARTICLE SIZE DISTRIBUTION.

4.2.2.1 Image Analysis.

An example of the three images generated by the Matlab R2018a are shown in Figure 19, 20 and 21. They refer to the sample at 0 min of digestion, after mastication.

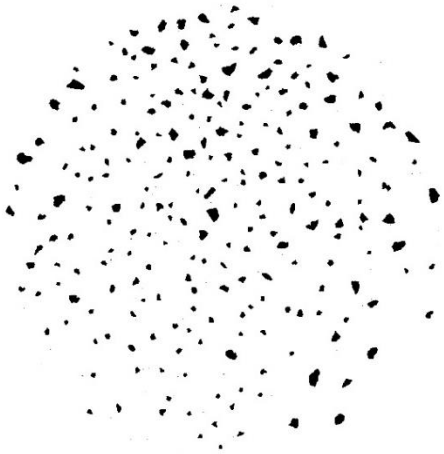

Figure 19. Image (B&W) generated by Matlab.

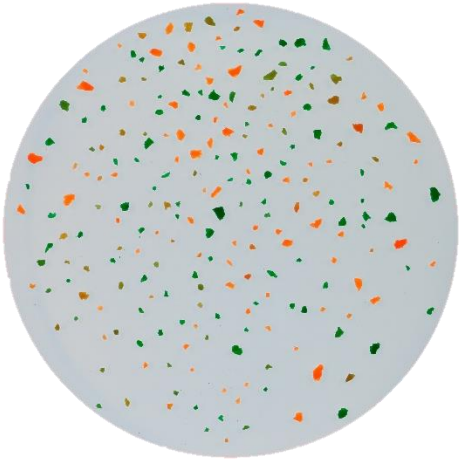

Figure 20. Image (Colorful) generated by Matlab.

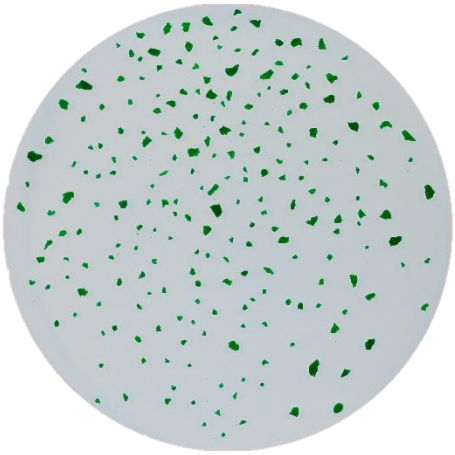

Figure 21. Image (Green) generated by Matlab.

B&W image determines what the program considers a particle. In addition, Colorful image determines what the program considers a different particle. In that way, if there are particles too close to others, they will count as a unique unit. Finally, Green image shows if any particle is hidden under another bigger.

The results also show that our food product has sufficient contrast with background. Consequently, the particles can be easily identified by the image processing algorithm.

Cumulative area distributions are given in Figure 22 for sweet potato crackers at 0 and 90 min of digestion.

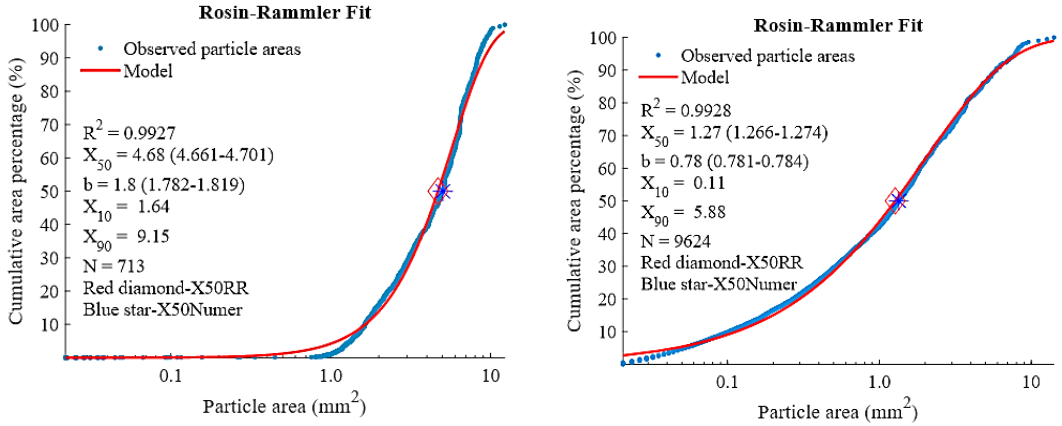

Figure 22. Rosin-Rammler plots for initial time point (0 min) (left) and after 90 min of digestion (right).

Rosin-Rammler model parameters and R^2 values during digestion are shown in Table 4. As can be noted by the large R^2 values (minimum of 0.9889) and the proximity of the observed data points to the predicted lines of the Rosin-Rammler model shown in Figure 22, the model fitted perfectly the particle properties. Moreover, pretty high b values (minimum of 0.78) indicate a narrow distribution of the particle sizes.

Time (min)	x_{50} (mm²)	b	R^2
0	4.68 ± 0.02	1.8 ± 0.02	0.9927
0.5	5.10 ± 0.03	1.49 ± 0.02	0.9889
30	4.06 ± 0.02	1.03 ± 0.01	0.9956
60	1.66 ± 0.01	0.84 ± 0.01	0.9967
90	1.27 ± 0.01	0.78 ± 0.01	0.9928
120	1.15 ± 0.01	0.78 ± 0.01	0.9927
150	1.08 ± 0.01	0.78 ± 0.01	0.9923

Table 4. Rosin-Rammler model parameters and R^2 values for sweet potato crackers over a 150 min digestion period.

The evolution of particle size distribution during the experiment is shown in Figure 23. Initial (0 min) and saliva (0.5 min) samples had a low particle size than the rest of the samples. That is a logical fact because they did not suffer any digestion process. Moreover, saliva sample particle size was bigger than the initial. That difference becomes explained by saliva absorption of the crackers during simulated oral digestion.

The smallest size of the particles belongs to the last timepoint of the digestion. Doubtless, that is because that sample was underwent to digestion for 150 min.

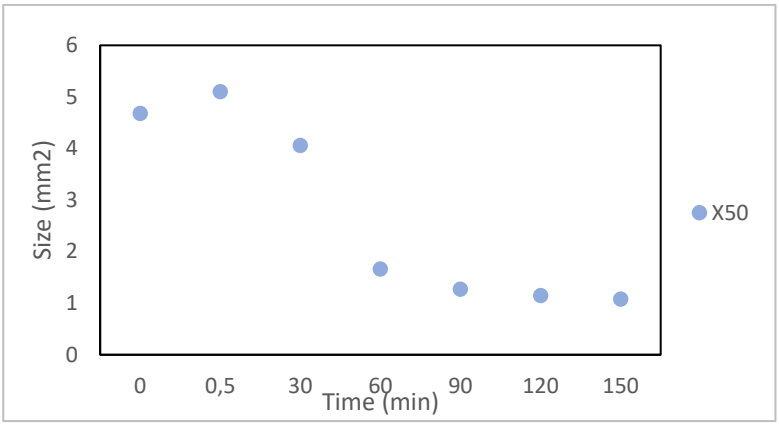

Figure 23. Medium average of particles in all the different time points for 2.5 hours digestion.

The number of particles per gram in all time points is shown in Figure 24. Initial (0 min) and saliva (0.5 min) samples reflect small number of particles in image analysis, logical fact because they did not suffer any alteration which could provoke their breakdown. Instead of that, image analysis of the different digestion timepoint samples detected a greater number of particles. That result reflects the breakdown process that occurs during digestion.

It is true that the number of particles would increase overtime. Nevertheless, due to the fact that there was not enough sample at the beginning of the digestion, at the last timepoints only liquid was collected. That is why the increase of number of particles stopped after 90 min. In the future the amount of SPC should be increased.

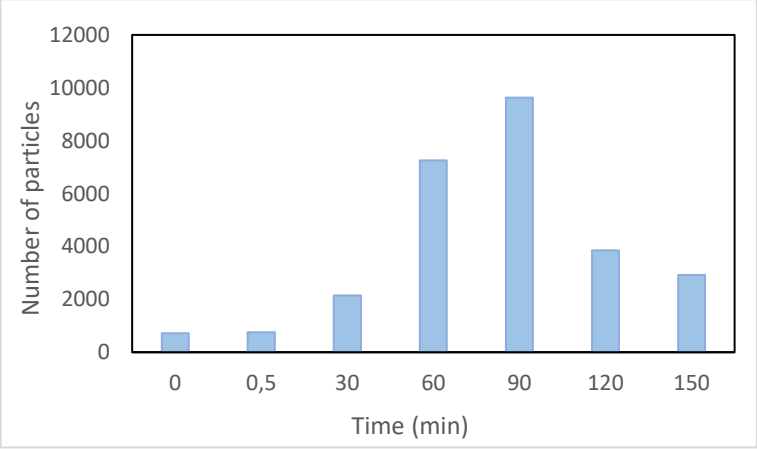

Figure 24. Number of particles per gram in all the different time points for 2.5 hours digestion.

The hypothesis for the number of particles per gram was that more digestion time implied a greater number of particles. In other words, during the different timepoints more amount of HCl was secreted into the stomach bag and due to that, the breakdown rate increased.

Moving on now to the medium average of particles, the hypothesis was that more digestion time implied smaller particles. As seen in Figure 23, it can be detected that smaller particles were determined during the end of the digestion.

4.2.2.2 Mastersizer 3000.

The medium particle size over time of the creamy layer is shown in Figure 25. Creamy layer appears after centrifuge the digested samples. For that reason, X axis starts at 30 minutes timepoint. As seen in Figure 25, even there is not too much difference, particle size of the creamy layer decreased during digestion. The result is explained by the same fact as image analysis, while breakdown increases, particle size decreases.

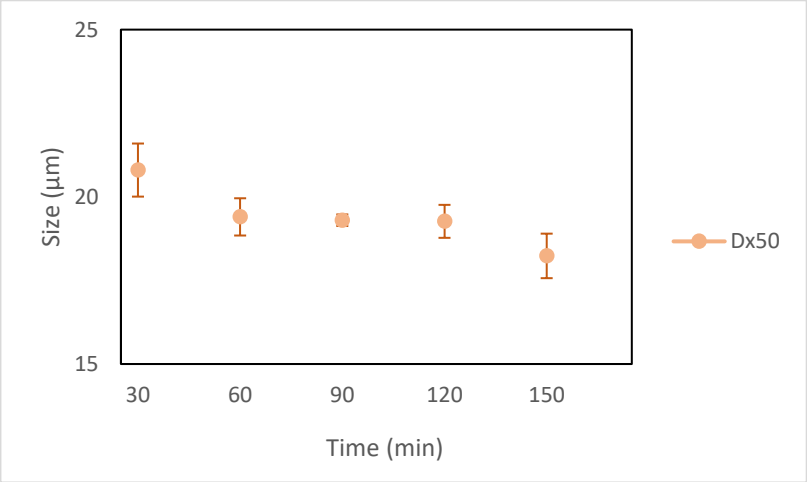

Figure 25. Creamy layer particle size of all the time points for 2.5 hours digestion.

5. CONCLUSIONS.

Overall, moisture content during digestion shows a clear rising trend in all treatments. Related to image analysis, the number of particles is greater at the end of the digestion and the area of particles is reduced from the initial sample to the final one. Both aspects are a result of the breakdown processes that occurs during digestion. In addition, particle size of the creamy layer also decreases during digestion as a result of the breakdown.

The results of this study showed that image analysis may be used to quantify the particle breakdown of a food product and it can also help to clarify the role of food structure and processing during gastric digestion.

In the future, the methods should be improved. To have enough representative sample for each timepoint, more than 120 g of sweet potato crackers should be used for the experiment. Another point is that image analysis should be done as soon as possible to avoid particles sticking.

Finally, after doing the experiments with all the different recipes and treatments, a comparison could be done between them in order to realize which one is the most digestible and to relate it to human body. The crux of the following studies will be how the different cooking methods and ingredients affect the digestion process.

6. REFERENCES.

Antia, B.S., Akpan, E.J., Okon, P.A., Umoren, I.U. (2006). Nutritive and Anti-Nutritive Evaluation of Sweet Potatoes (Ipomoea batatas) Leaves. *Pakistan Journal of Nutrition*, 5(2), pp.166-168.

Barrett KE. (2005). Gastrointestinal physiology. Lange physiology series: McGraw-Hill, Columbus (OH).

Benini, L., Castellani, G., Brighenti, F., Heaton, K.W., Brentegani, M.T., Casiraghi, M.C., Sembenini, C., Pellegrini, N., Fioretta, A., Minniti, G. (1995). Gastric emptying of a solid meal is accelerated by the removal of dietary fiber naturally present in food. *Gut.* 36(6), pp.825–30.

Bornhorst, G. M. (2017). Gastric Mixing During Food Digestion: Mechanisms and Applications. *Annual Review of Food Science and Technology*, 8(1), pp. 523–542.

Bornhorst, G.M., Singh, R.P. (2012). Bolus Formation and Disintegration during Digestion of Food Carbohydrates. *Comprehensive Reviews in Food Science and Food Safety*, 11(2), pp.101–118.

Bornhorst, G., Ferrua, M., Singh, R. (2015). A Proposed Food Breakdown Classification System to Predict Food Behavior during Gastric Digestion. *Journal of Food Science*, 80(5), pp.924-934.

Bornhorst, G.M., Singh, R.P. (2013). Kinetics of in vitro bread bolus digestion with varying oral and gastric digestion parameters. *Food Biophys*. 8 (1), pp.50-59.

Bornhorst, G. M., Singh, R.P. (2014). Gastric Digestion In Vivo and In Vitro: How the Structural Aspects of Food Influence the Digestion Process. *Annual Review of Food Science and Technology*, 5(1), pp.111–132.

Bornhorst, G. M., Gouseti, O., Wickham, M. S. J., & Bakalis, S. (2016). Engineering Digestion: Multiscale Processes of Food Digestion. *Journal of Food Science*, 81(3), pp.534–543

Bornhorst, G., Kostlan, K., Singh, R. (2013). Particle Size Distribution of Brown and White Rice during Gastric Digestion Measured by Image Analysis. *Journal of Food Science*, 78(9), pp. 1383-1391.

Bovell-Benjamin, A.C. (2007). Sweet potato: a review of its past, present, and future role in human nutrition. *Advances in Food and Nutrition Research.* 52, pp.1–59.

Burri, B. J. (2011). Evaluating Sweet Potato as an Intervention Food to Prevent Vitamin A Deficiency. *Comprehensive Reviews in Food Science and Food Safety*, 10(2), pp. 118–130.

Di Mario, F. and Goni, E. (2014). Gastric acid secretion: Changes during a century. *Best Practice & Research Clinical Gastroenterology*, 28(6), pp.953-965.

Drechsler, K., Ferrua, M. (2016). Modelling the breakdown mechanics of solid foods during gastric digestion. *Food Research International*, 88, pp.181-190.

Dressman et al., (1990) Upper gastrointestinal (GI) pH in young, healthy men and women. Pharm. Res. 7, pp.756–761.

Guo, Q., Ye, A., Lad, M., Dalgleish, D., Singh, H. (2014). Effect of gel structure on the gastric digestion of whey protein emulsion gels. *Soft Matter*, 10(8), p.1214.

Hersey, S. J., & Sachs, G. (1995). Gastric acid secretion. Physiological Reviews, 75(1), pp.155–189.

Hertog M.G.L, Feskens E.J.M, Kromhout D, Hollman P.C.H, Katan M.B. (1993). Dietary antioxidant flavonoids and risk of coronary heart disease: the Zutphen Elderly Study. *Lancet.* 342 (8878), pp.1007.

Jalabert-Malbos, M., Mishellany-Dutour, A., Woda, A. and Peyron, M. (2007). Particle size distribution in the food bolus after mastication of natural foods. *Food Quality and Preference*, 18(5), pp.803-812.

Kelly, K.A. (1980). Gastric emptying of liquids and solids: roles of proximal and distal stomach. *Am J Physiol Gastrointest Liver Physiol* 239(2): G 71-6.

Kwiatek, M. A., Fox, M. R., Steingoetter, A., Menne, D., Pal, A., Fruehauf, H., Schwizer, W. (2009). Effects of clonidine and sumatriptan on postprandial gastric volume response, antral contraction waves and emptying: an MRI study. *Neurogastroenterology and Motility*, 21(9), pp. 928-71.

Lammers, W., Ver Donck, L., Stephen, B., Smets, D. and Schuurkes, J. (2009). Origin and propagation of the slow wave in the canine stomach: the outlines of a gastric conduction system. *American Journal of Physiology-Gastrointestinal and Liver Physiology*, 296(6), pp. 1200-1210.

Malagelada, J., Longstreth, G., Summerskill, W. and Go, V. (1976). Measurement of Gastric Functions During Digestion of Ordinary Solid Meals in Man. *Gastroenterology*, 70(2), pp.203-210.

Marciani, L., Gowland, P., Spiller, R., Manoj, P., Moore, R., Young, P. and Fillery-Travis, A. (2001). Effect of meal viscosity and nutrients on satiety, intragastric dilution, and emptying assessed by MRI. *American Journal of Physiology-Gastrointestinal and Liver Physiology*, 280(6), pp.1227-1233.

Mennah-Govela, Y. and Bornhorst, G. (2016). Acid and moisture uptake in steamed and boiled sweet potatoes and associated structural changes during in vitro gastric digestion. *Food Research International*, 88, pp.247-255.

Mennah-Govela, Y.A., Bornhorst, G.M., Singh, R.P. (2015). Acid diffusion into rice boluses is influenced by rice type, variety, and presence of a-amylase. *Journal of Food Science*. 80 (2), pp.316-325

Mennah-Govela, Y.A, Bornhorst, G.M. (2016). Mass transport processes in orange-fleshed sweet potatoes leading to structural changes during in vitro gastric digestion. *Journal of Food Engineering*, 191, pp.48-57.

Meyer, J.H. (1980). Gastric emptying of ordinary food: effect of antrum on particle size. *Am J Physiol Gastrointest Liver Physiol* 239(3): G 133–5.

Minekus, M., Alminger, M., Alvito, P., Ballance, S., Bohn, T., Bourlieu, C., . . . Dupont, D. (2014). A standardised static in vitro digestion method suitable for food–an international consensus. *Food & Function*, 5(6), pp.1113-1124.

Roman, M. J., Burri, B. J., & Singh, R. P. (2012). Release and bioaccessibility of beta-carotene from fortified almond butter during in vitro digestion. *Journal of Agricultural and Food Chemistry*, 60(38), pp.9659-9666.

Tai-Hua Mu, Hong-Nan Sun, Meng-Mei Ma. (2019). Sweet potato snack foods. *Sweet Potato Academic Press*, 11, pp.303-324.

Teow, C., Truong, V., McFeeters, R., Thompson, R., Pecota, K., Yencho, G. (2007). Antioxidant activities, phenolic and β-carotene contents of sweet potato genotypes with varying flesh colours. *Food Chemistry*, 103(3), pp.829-838.

Thomas A. (2006). Gut motility, sphincters and reflex control. *Anesthesia Intense Care Med* 7(2): pp.57–8.

Wang, S., Nie, S., Zhu, F. (2016). Chemical constituents and health effects of sweet potato. *Food Research International*, 89, pp.90–116.

Wilson, C. D., Pace, R. D., Bromfield, E., Jones, G., and Lu, J. Y. (1998). Sweet potato in a vegetarian menu plan for NASA's advanced life support program.

Witt, T., Stokes, J. (2015). Physics of food structure breakdown and bolus formation during oral processing of hard and soft solids. *Current Opinion in Food Science*, 3, pp.110-117.

Woolfe, J.A. (1992). Sweet Potato: An Untapped Food Resource. *Cambridge University Press* (1992), pp. 643.

7. ANNEXES.

Annex 1. Study of the crackers overtime stability.

In order to check the stability of the product and to know if the crackers could be made more in advance, their initial properties were analyzed for 4 days.

- No protein crackers.

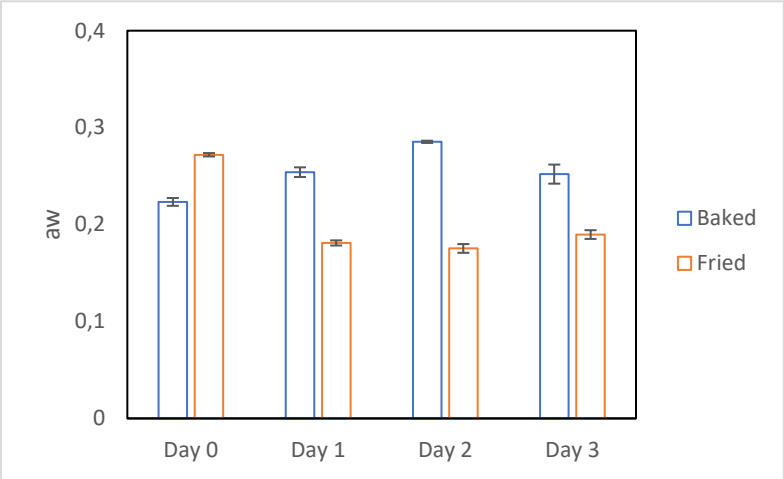

Figure 26. Water activity of no protein crackers overtime.

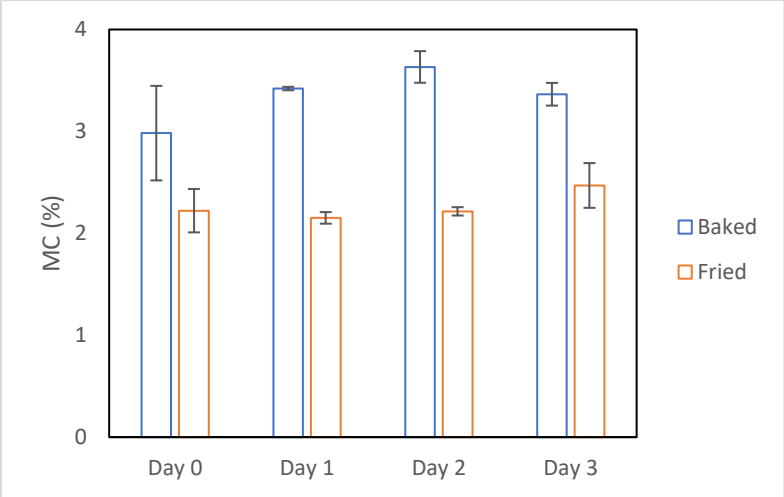

Figure 27. Moisture content of no protein crackers overtime.

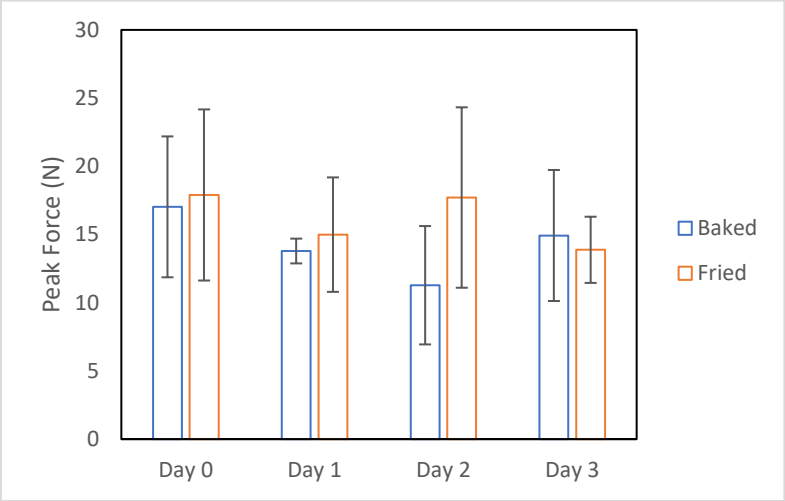

Figure 28. Texture of no protein crackers overtime.

- Hydrolyzed egg protein crackers.

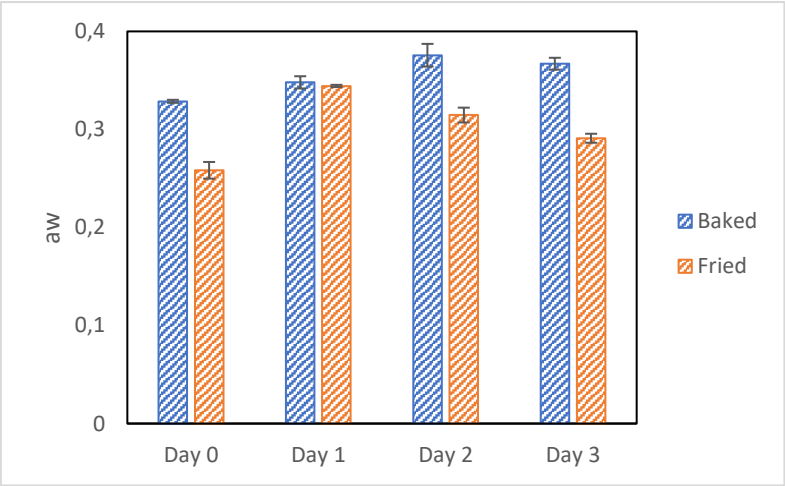

Figure 29. Water activity of hydrolyzed egg protein crackers overtime.

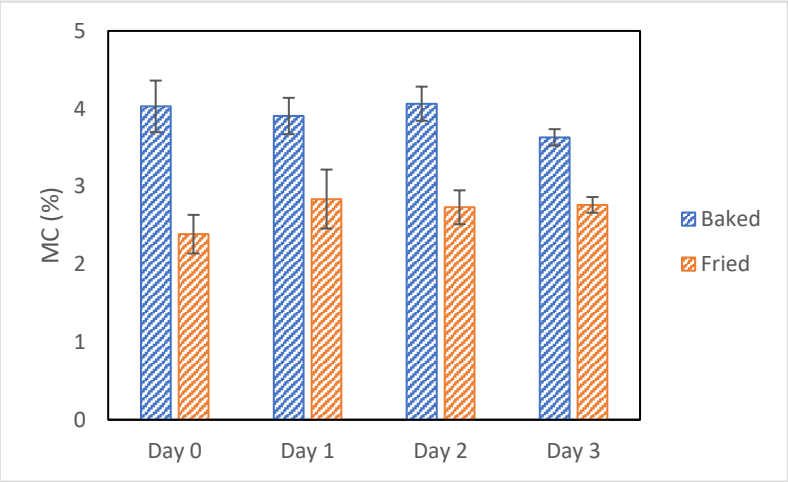

Figure 30. Moisture content of hydrolyzed egg protein crackers overtime.

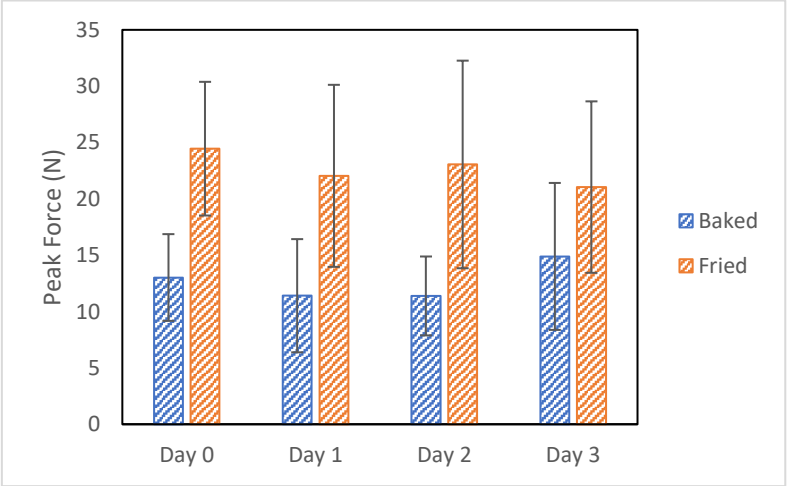

Figure 31. Texture of hydrolyzed egg protein crackers overtime.

- Pea protein crackers.

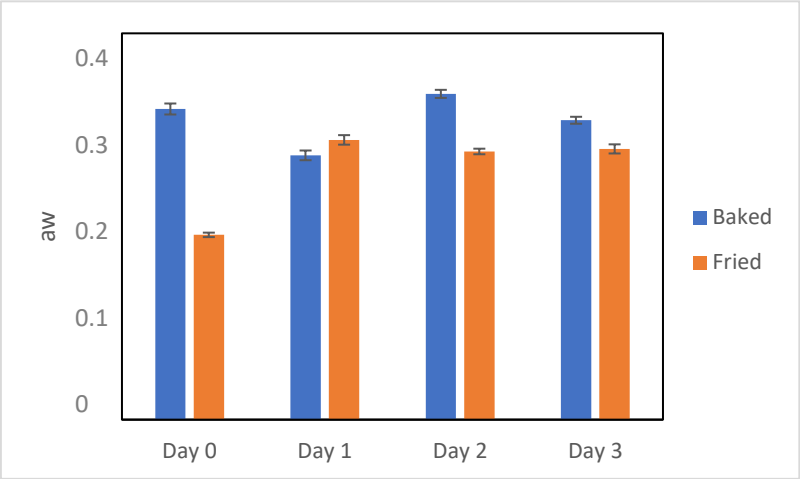

Figure 31. Water activity of pea protein crackers overtime.

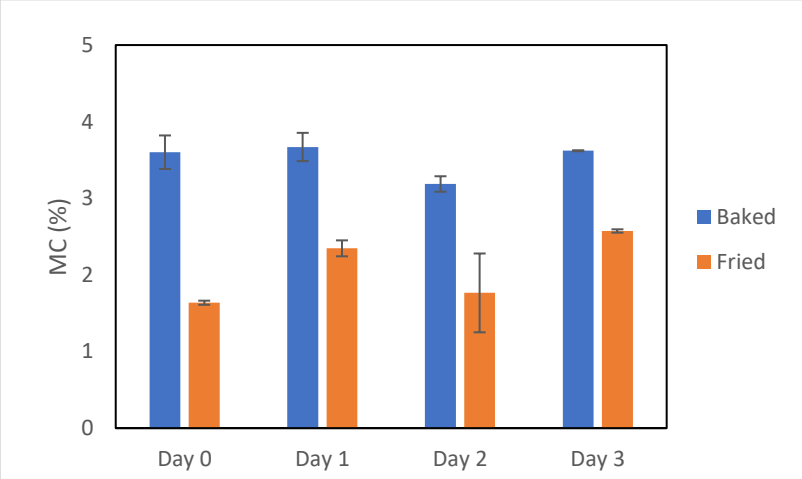

Figure 32. Moisture content of pea protein crackers overtime.

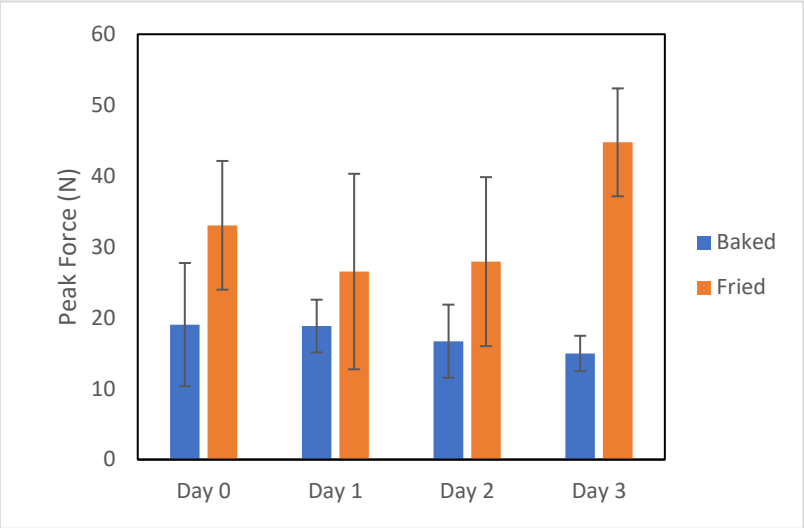

Figure 34. Texture of pea protein crackers overtime.

As observed on the graphs, values do not change excessively so the crackers could be made ahead of time. Nevertheless, it is recommended not to surpass more than 2 days in order to maintain all their properties.